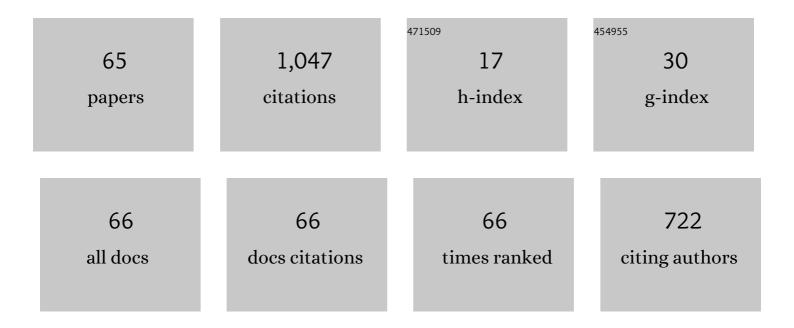
List of Publications by Year in descending order

Source: https://exaly.com/author-pdf/4167942/publications.pdf Version: 2024-02-01



LUNYA INOUE

#	Article	IF	CITATIONS
1	Fracture elongation of brittle/ductile multilayered steel composites with a strong interface. Scripta Materialia, 2008, 59, 1055-1058.	5.2	188
2	Transition in deformation behavior of martensitic steel during large deformation under uniaxial tensile loading. Scripta Materialia, 2009, 60, 221-224.	5.2	121
3	Development of Multilayer Steels for Improved Combinations of High Strength and High Ductility. Materials Transactions, 2014, 55, 227-237.	1.2	101
4	Slip band formation at free surface of lath martensite in low carbon steel. Acta Materialia, 2019, 165, 129-141.	7.9	38
5	Interphase Strain Gradients in Multilayered Steel Composite from Microdiffraction. Metallurgical and Materials Transactions A: Physical Metallurgy and Materials Science, 2014, 45, 98-108.	2.2	34
6	Data assimilation for massive autonomous systems based on a second-order adjoint method. Physical Review E, 2016, 94, 043307.	2.1	34
7	High stereographic resolution texture and residual stress evaluation using time-of-flight neutron diffraction. Journal of Applied Crystallography, 2018, 51, 746-760.	4.5	27
8	Shared computer-aided structural design model for construction industry (infrastructure). CAD Computer Aided Design, 2008, 40, 778-788.	2.7	26
9	Prediction of Ac ₃ and Martensite Start Temperatures by a Data-driven Model Selection Approach. ISIJ International, 2017, 57, 2229-2236.	1.4	26
10	Stochastic characterization and reconstruction of material microstructures for establishment of process-structure-property linkage using the deep generative model. Physical Review E, 2021, 104, 025302.	2.1	25
11	Solidification of Iron and Steel on Single-crystal Oxide. ISIJ International, 2007, 47, 847-852.	1.4	22
12	Reactive Transient Liquid Phase Bonding between AZ31 Magnesium Alloy and Low Carbon Steel. Materials Transactions, 2011, 52, 568-571.	1.2	20
13	Strain localization behavior in low-carbon martensitic steel during tensile deformation. Scripta Materialia, 2013, 69, 793-796.	5.2	19
14	Grain growth prediction based on data assimilation by implementing 4DVar on multi-phase-field model. Science and Technology of Advanced Materials, 2017, 18, 857-868.	6.1	19
15	Unsupervised microstructure segmentation by mimicking metallurgists' approach to pattern recognition. Scientific Reports, 2020, 10, 17835.	3.3	19
16	Void formation in nanocrystalline Cu film during uniaxial relaxation test. Acta Materialia, 2008, 56, 4921-4931.	7.9	18
17	Crystallographic and Microstructural Studies of Lath Martensitic Steel During Tensile Deformation. Metallurgical and Materials Transactions A: Physical Metallurgy and Materials Science, 2014, 45, 5029-5043.	2.2	18
18	Laminated Metal Composites by Infiltration. Metallurgical and Materials Transactions A: Physical Metallurgy and Materials Science, 2011, 42, 3509-3520.	2.2	17

#	Article	IF	CITATIONS
19	Ferrite transformation from oxide–steel interface in HAZ-simulated C–Mn steel. International Journal of Materials Research, 2008, 99, 347-351.	0.3	15
20	Ferrite Formation Behaviors from B1 Compounds in Steels. ISIJ International, 2011, 51, 2036-2041.	1.4	15
21	Transformation Behavior of Ferrite at Steel/B1 Compounds Interface. Tetsu-To-Hagane/Journal of the Iron and Steel Institute of Japan, 2010, 96, 123-128.	0.4	14
22	Effects of Solute Carbon on the Work Hardening Behavior of Lath Martensite in Low-Carbon Steel. ISIJ International, 2017, 57, 181-188.	1.4	14
23	Flow analysis of jointed rock masses based on excavation-induced transmissivity change of rough joints. International Journal of Rock Mechanics and Minings Sciences, 2004, 41, 959-974.	5.8	13
24	Effect of Stress on Variant Selection in Lath Martensite in Low-carbon Steel. ISIJ International, 2013, 53, 1453-1461.	1.4	13
25	Fracture Toughness of Fe-Zn Intermetallic Compound Layer. Tetsu-To-Hagane/Journal of the Iron and Steel Institute of Japan, 2014, 100, 383-389.	0.4	13
26	Bonding Interface Formation between Mg Alloy and Steel by Liquid-phase Bonding using the Ag Interlayer. Metallurgical and Materials Transactions A: Physical Metallurgy and Materials Science, 2012, 43, 592-597.	2.2	12
27	Fracture Toughness Evaluation of Thin Fe–Al Intermetallic Compound Layer at Reactive Interface between Dissimilar Metals. Materials Transactions, 2013, 54, 994-1000.	1.2	12
28	In situ deformation analysis of Mg in multilayer Mg-steel structures. Materials and Design, 2017, 119, 326-337.	7.0	11
29	Effect of initial texture and microstructure of Mg on mechanical properties of Mg – Stainless steel laminated metal composites. Materials Characterization, 2017, 127, 171-178.	4.4	9
30	A simple method for measurement of shear delamination toughness in environmental barrier coatings. Surface and Coatings Technology, 2017, 321, 213-218.	4.8	9
31	Bayesian inference of ferrite transformation kinetics from dilatometric measurement. Computational Materials Science, 2020, 184, 109837.	3.0	9
32	In-situ measurement of surface relief induced by Widmanstäten and bainitic ferrites in low carbon steel by digital holographic microscopy. Scripta Materialia, 2019, 162, 241-245.	5.2	8
33	Development of Data-Driven System in Materials Integration. Materials Transactions, 2020, 61, 2058-2066.	1.2	8
34	Establishment of structure-property linkages using a Bayesian model selection method: Application to a dual-phase metallic composite system. Acta Materialia, 2019, 176, 264-277.	7.9	7
35	Bayesian inference of grain growth prediction via multi-phase-field models. Physical Review Materials, 2019, 3, .	2.4	7
36	Analytical Study for Deformability of Laminated Sheet Metal with Full Interfacial Bond. Journal of Engineering Mechanics - ASCE, 2013, 139, 94-103.	2.9	6

#	Article	IF	CITATIONS
37	Effect of Si Content in Steel on Formation of Fe-Zn Intermetallic Compound Layer at Pure Zn Melt/Steel Interface. Tetsu-To-Hagane/Journal of the Iron and Steel Institute of Japan, 2014, 100, 390-396.	0.4	6
38	Fracture Behavior of Multi-phase Fe-Zn Intermetallic Compound Layer. Tetsu-To-Hagane/Journal of the Iron and Steel Institute of Japan, 2016, 102, 714-721.	0.4	6
39	Multilayer Mg-Stainless Steel Sheets, Microstructure, and Mechanical Properties. Metallurgical and Materials Transactions A: Physical Metallurgy and Materials Science, 2017, 48, 2483-2495.	2.2	6
40	ESTIMATION OF HYDRAULIC PROPERTY OF JOINTED ROCK MASS CONSIDERING EXCAVATION-INDUCED CHANGE IN PERMEABILITY OF EACH JOINTS. Soils and Foundations, 2005, 45, 43-59.	0.7	6
41	In-situ Observation of Ferrite Plate Formation in Low Carbon Steel during Continuous Cooling Process. Tetsu-To-Hagane/Journal of the Iron and Steel Institute of Japan, 2008, 94, 363-368.	0.4	5
42	Unsupervised segmentation of microstructural images of steel using data mining methods. Computational Materials Science, 2022, 201, 110855.	3.0	5
43	An integrated approach for numerically predicting the failure of resistance spot welds. Science and Technology of Welding and Joining, 2022, 27, 229-237.	3.1	5
44	Distributed object-based software environment for urban system integrated simulation under urban-scale hazard—Part II: Application. Earthquake Engineering and Structural Dynamics, 2007, 36, 1561-1579.	4.4	4
45	Distributed object-based software environment for urban system integrated simulation under urban-scale hazard—Part I: Infrastructure. Earthquake Engineering and Structural Dynamics, 2007, 36, 1545-1560.	4.4	4
46	Phase Evolution During the Liquid-Phase Bonding of Zirconium and Austenitic Stainless Steel with Zinc Insertion. Metallurgical and Materials Transactions A: Physical Metallurgy and Materials Science, 2012, 43, 2366-2377.	2.2	4
47	Effect of Stress on Variant Selection of Lath Martensite in Low-carbon Steel. Tetsu-To-Hagane/Journal of the Iron and Steel Institute of Japan, 2012, 98, 425-433.	0.4	4
48	Bayesian inverse design of high-strength aluminum alloys at high temperatures. MRS Advances, 2022, 7, 213-216.	0.9	4
49	Hierarchical Localization of Sensor Network for Infrastructure Monitoring. Journal of Infrastructure Systems, 2008, 14, 15-26.	1.8	3
50	Yet another possible mechanism for anomalous transport: Theory, numerical method, and experiments. KSCE Journal of Civil Engineering, 2012, 16, 45-53.	1.9	3
51	Crystallographic Analysis of Transformation Behavior of Acicular Ferrite from B1-type Compounds in Steels. ISIJ International, 2017, 57, 1246-1251.	1.4	2
52	Hierarchical Localization Algorithm Based on Inverse Delaunay Tessellation. Lecture Notes in Computer Science, 2006, , 180-195.	1.3	2
53	Development of Data-Driven System in Materials Integration. Materia Japan, 2019, 58, 503-510.	0.1	2
54	Effects of Solute Carbon on the Work Hardening Behavior of Lath Martensite in Low-Carbon Steel. Tetsu-To-Hagane/Journal of the Iron and Steel Institute of Japan, 2020, 106, 488-496.	0.4	2

#	Article	IF	CITATIONS
55	Radiation-Induced Surface Wettability Enhancement of an Indium Tin Oxide and Titanium Oxide Film-Coated Sapphire. Journal of Nuclear Engineering and Radiation Science, 2022, 8, .	0.4	1
56	Development of Digital Holographic Microscope for <i>In-Situ</i> Surface Relief Measurement of Low-Carbon Steel. Materials Transactions, 2020, 61, 42-48.	1.2	1
57	Creep Life Predictions by Machine Learning Methods for Ferritic Heat Resistant Steels. Tetsu-To-Hagane/Journal of the Iron and Steel Institute of Japan, 2022, 108, 424-437.	0.4	1
58	Mechanical Behavior of Nanocrystalline Cu Alloy Thin Film on Elastomer Substrates Under Constant Uniaxial Tensile Strain. Materials Research Society Symposia Proceedings, 2006, 976, 1.	0.1	0
59	DEVELOPMENT OF HIERARCHICAL SENSOR NETWORK SYSTEM FOR INFRASTRUCTURE MONITORING. Doboku Gakkai Ronbunshuu A, 2008, 64, 82-100.	0.3	0
60	Steel-Magnesium Laminated Composites by Infiltration. Materials Research Society Symposia Proceedings, 2012, 1373, 143.	0.1	0
61	Multilayer Mg–Stainless Steel Sheets, Twinning and Texture Evolution. Metallurgical and Materials Transactions A: Physical Metallurgy and Materials Science, 2017, 48, 3514-3522.	2.2	0
62	Numerical studies of the effect of residual imperfection on the mechanical behavior of heat-corrected steel plates, and analysis of a further repair method. Steel and Composite Structures, 2009, 9, 209-221.	1.3	0
63	134 Data assimilation for massive simulation models: in the case of the phase field model. The Proceedings of the Computational Mechanics Conference, 2015, 2015.28, _134-1134-2	0.0	0
64	Local Deformation Analysis in Martensite Layer of High-Strength Multilayered Steel Composite Using Synchrotron X-ray Diffraction. Zairyo/Journal of the Society of Materials Science, Japan, 2017, 66, 420-426.	0.2	0
65	<i>In-situ</i> Measurement of Bainitic Transformation Process using Digital Holographic Microscope. Tetsu-To-Hagane/Journal of the Iron and Steel Institute of Japan, 2022, 108, 360-369.	0.4	0